DnaJ Dramatically Stimulates ATP Hydrolysis by DnaK: Insight into Targeting of Hsp70 Proteins to Polypeptide Substrates†

Rick Russell,‡ A. Wali Karzai,§ Andrew F. Mehl,|| and Roger McMacken*

Department of Biochemistry, Johns Hopkins University, School of Hygiene and Public Health, Baltimore, Maryland 21205

Received September 23, 1998; Revised Manuscript Received January 29, 1999

ABSTRACT: Most, if not all, of the cellular functions of Hsp70 proteins require the assistance of a DnaJ homologue, which accelerates the weak intrinsic ATPase activity of Hsp70 and serves as a specificity factor by binding and targeting specific polypeptide substrates for Hsp70 action. We have used pre-steady-state kinetics to investigate the interaction of the *Escherichia coli* DnaJ and DnaK proteins, and the effects of DnaJ on the ATPase reaction of DnaK. DnaJ accelerates hydrolysis of ATP by DnaK to such an extent that ATP binding by DnaK becomes rate-limiting for hydrolysis. At high concentrations of DnaK under single-turnover conditions, the rate-limiting step is a first-order process, apparently a change of DnaK conformation, that accompanies ATP binding and proceeds at 12−15 min^{-1} at 25 °C and 1−1.5 min^{-1} at 5 °C. By prebinding ATP to DnaK and subsequently adding DnaJ, the effects of this slow step may be bypassed, and the maximal rate-enhancement of DnaJ on the hydrolysis step is ∼15 000-fold at 5 °C. The interaction of DnaJ with DnaK·ATP is likely a rapid equilibrium relative to ATP hydrolysis, and is relatively weak, with a K_D of ∼20 μM at 5 °C, and weaker still at 25 °C. In the presence of saturating DnaJ, the maximal rate of ATP hydrolysis by DnaK is similar to previously reported rates for peptide release from DnaK·ATP. This suggests that when DnaK encounters a DnaJ-bound polypeptide or protein complex, a significant fraction of such events result in ATP hydrolysis by DnaK and concomitant capture of the polypeptide substrate in a tight complex with DnaK·ADP. Furthermore, a broadly applicable kinetic mechanism for DnaJ-mediated specificity of Hsp70 action arises from these observations, in which the specificity arises largely from the acceleration of the hydrolysis step itself, rather than by DnaJ-dependent modulation of the affinity of Hsp70 for substrate polypeptides.

DnaK is a constitutively expressed *Escherichia coli* member of the highly conserved heat shock protein 70 (Hsp70)[1] family of molecular chaperones. In addition to protecting proteins from denaturation caused by heat or certain other forms of stress, Hsp70 proteins have been shown to function in various aspects of protein metabolism, including synthesis and folding of nascent polypeptides, intracellular protein trafficking, and protein degradation [(*1*−*5*); for recent reviews, see (*6*, *7*)]. Additionally, Hsp70 proteins participate in the disassembly of specific protein and nucleoprotein complexes. For example, Hsc70, a constitutively expressed form of eukaryotic Hsp70, removes clathrin from endocytic vesicles (*8*, *9*). DnaK is required for the initiation of DNA replication in some phages, including λ (*10*, *11*) and P1 (*12*), where in both cases DnaK mediates disassembly of protein complexes formed prior to replication initiation.

In all of these processes, Hsp70s are thought to function by undergoing repetitive association/dissociation cycles, first binding and later releasing polypeptide substrates. Structural analyses have shown that short synthetic peptides bind to the C-terminal domain of Hsp70 in an extended conformation (*13*, *14*), which likely mimics the binding of physiological substrates. These cycles of polypeptide binding and release are coupled to the ATP binding and hydrolysis activities associated with Hsp70 proteins. These latter activities have been localized to the Hsp70 N-terminal domain (*15*−*17*). The ATP-bound state of Hsp70 is characterized by relatively weak binding of polypeptides, with rapid rates of association and dissociation [k_{off} = 1−3 s^{-1} (*18*−*20*)]. The intrinsic rate of ATP hydrolysis is very slow [0.02 min^{-1} at 25 °C for DnaK (*21*, *22*)], but polypeptides stimulate this activity up to ∼25-fold (*20*, *23*). Conversion of Hsp70 to the ADP-bound form through hydrolysis dramatically decreases the dissociation rate of peptides and results in the formation of a relatively stable Hsp70·ADP·polypeptide complex (*24*). Completion of the catalytic cycle requires, sequentially, release of ADP and rebinding of ATP. It is this latter event that provokes the rapid dissociation of bound polypeptide from Hsp70 (*25*).

† This research was supported by NIH Grant GM36526 from the National Institute of General Medical Sciences. R.R. was supported in part by NIEHS Training Grant ES07141.

* To whom correspondence should be addressed. Telephone: 410-955-3949. Fax: 410-955-2926. E-mail: rmcmacken@jhsph.edu.

‡ Present address: Department of Biochemistry, Stanford University, Stanford, CA 94305.

§ Present address: Department of Biology, Massachusetts Institute of Technology, Cambridge, MA 02139.

|| Present address: Department of Chemistry, Knox College, Galesburg, IL 61401.

[1] Abbreviations: Hsp70, heat shock protein 70; Hsc70, heat shock cognate 70; P_i, inorganic phosphate; Hepes, 4-(2-hydroxyethyl)-piperazine-1-ethanesulfonic acid; ATP*, [α-^{32}P]ATP; ADP*, [α-^{32}P]ADP; K^+Glu^-, potassium glutamate; GAP, GTPase-activating protein.

10.1021/bi9824036 CCC: $18.00
Published on Web 03/11/1999

While the ATPase activity controls the polypeptide binding cycle, the DnaK ATPase cycle is itself controlled by the DnaJ and GrpE cochaperone regulatory proteins in *E. coli*. These proteins affect the rates of specific steps in the ATPase cycle. DnaJ increases the ATP hydrolysis rate (*26*) at least 200-fold (*27*), favoring the ADP-bound state of DnaK. GrpE, on the other hand, "recycles" DnaK by increasing the dissociation rate of ADP (*26*, *28*), favoring the ATP-bound state. An additional function of DnaJ is to confer specificity to the action of DnaK by binding certain protein complexes and targeting them for DnaK (*29*−*31*). Targeting by DnaJ may in fact be a general requirement for DnaK action, as DnaJ has been shown to bind polypeptides emerging from the ribosome (*32*).

Like Hsp70s, DnaJ homologues are present in eukaryotic cells in virtually every subcellular organelle, and in several cases these proteins have been shown to interact with Hsp70s both in vitro (*33*, *34*) and in vivo (*35*, *36*). Because DnaJ proteins are modular in design, the extent of homology between *E. coli* DnaJ and eukaryotic homologues is highly variable. While all family members contain a "J-domain," which has been shown to be essential for stimulation of DnaK's ATPase activity (*27*, *37*), some eukaryotic proteins contain little or no additional homology. Still others are conserved over the entire length of the amino acid sequence. An example of the former case is the yeast endoplasmic reticulum membrane protein Sec63p, which contains a lumenal J-domain but bears no other resemblance to DnaJ (*38*). Nevertheless, the functional properties of Sec63p share remarkable similarities to those of DnaJ. Sec63p is required for polypeptide transport into the endoplasmic reticulum in a process that is also dependent on a lumenal Hsp70 protein (*39*). Moreover, both biochemical (*34*) and genetic (*35*, *40*) interactions between the two proteins have been demonstrated. In certain cases, substrate binding by DnaJ and DnaJ-like proteins has been localized to sequences away from the J-domain (*41*, *42*). For example, the clathrin binding site of auxilin, a 99 kDa protein which contains a J-domain and is required for Hsc70-mediated uncoating of clathrin-coated vesicles, has been localized to a 268-amino acid region adjacent to the J-domain (*43*). From these and other results, a model has emerged wherein the J-domain serves to recruit Hsp70 to sites of action dictated by the substrate binding domain(s) of the DnaJ-like protein (*27*, *44*, *45*). Because the substrate binding domains of DnaJ homologues vary significantly, this may account for the broad nature of the substrates upon which Hsp70 proteins act. However, the process by which this targeting occurs is not clearly understood.

In this report, we have used a kinetic approach to further investigate the interaction of *E. coli* DnaJ and DnaK and the effects of DnaJ on the ATP hydrolysis reaction of DnaK. These studies have revealed that the stimulation by DnaJ is much greater than was previously thought, ~15 000-fold at 5 °C, and is such that a change in the rate-limiting step occurs as the DnaJ concentration is increased. Single-turnover ATPase reactions are rate-limited at high concentrations of DnaJ by a first-order step associated with the binding of ATP to DnaK. We have also determined that the affinity of DnaJ for the DnaK·ATP complex is quite weak ($K_D^J \approx 20\ \mu$M). Taken together with previous findings, our results suggest a model whereby the polypeptide target specificity conferred by DnaJ upon DnaK arises in large measure from its capacity to elicit a tremendous acceleration of ATP hydrolysis by DnaK.

MATERIALS AND METHODS

Materials. Materials and their sources were as follows: poly(ethylenimine)−cellulose thin-layer chromatography sheets, EM Industries; ATP, Pharmacia Biotech; ADP, Calbiochem; [α-^{32}P]ATP (ATP*; >3000 Ci/mmol), Amersham. All other biochemicals were from Sigma Chemical Co.

Expression and Purification of Proteins. DnaK and DnaJ were expressed and purified as described (*22*, *27*). For experiments in which observed rate constants or stoichiometries of hydrolysis were expected to be dependent on the concentration of free DnaK, endogenous nucleotide was removed (*22*). *E. coli* GrpE protein was purified to near-homogeneity from cells carrying amplified levels of this cochaperone. The construction of the GrpE-overproducing clone and a modified purification protocol for GrpE will be described elsewhere (A. Mehl, unpublished results).

Determination of Protein Concentration. The concentrations of DnaK and DnaJ were determined spectrophotometrically as described (*23*, *27*), using the calculated molar extinction coefficient of 15 800 M^{-1} cm^{-1} for DnaK, and the value of 14 000 M^{-1} cm^{-1} for DnaJ, determined by the method of Gill and von Hippel (*46*).

General Kinetic Methods. Unless indicated otherwise, experiments were carried out under single-turnover conditions, with DnaK present in large excess over ATP* (*22*). The standard reaction buffer (HM buffer) was 40 mM Hepes/KOH, pH 7.6, 11 mM magnesium acetate, and 200 mM potassium glutamate (K^+Glu^-). Time courses of ATP hydrolysis were performed either by initiating the reaction with the addition of ATP* to DnaK, or by preincubating DnaK with ATP* (during which time hydrolysis of ATP is very slow) and initiating with DnaJ. Portions of the reaction mixture were quenched with HCl, and the fraction of labeled material converted to [α-^{32}P]ADP (ADP*) was determined by thin-layer chromatographic separation of ATP* from ADP*, followed by quantitation using a Fuji Bas 1000 imager. Reactions were typically followed for ≥4 half-lives, and uncorrected end points were found to be ~90% (see below). Reactions measuring the intrinsic ATPase rate of DnaK at 5 °C were followed to ~35% completion (8 h), and an end point of 90% was assumed.

Rapid Time Scale Kinetic Experiments. Reactions that occurred too rapidly to measure by hand (<10 s) were monitored using a Kintek RQF-3 rapid quench-flow apparatus (*47*, *48*). Proteins and ATP* were loaded into separate 1 mL syringes which were used to fill the 15 μL sample loops. The drive syringes were pushed at a constant velocity, mixing the sample solutions in a 1:1 ratio. The reactions were automatically quenched after a defined reaction time (0.05−120 s) with 80 μL of a 0.3 N HCl solution present in a separate drive syringe.

For reactions in which DnaK was preincubated with ATP* prior to initiation of the reaction by addition of DnaJ, DnaK and ATP* were mixed at a defined time and loaded into a 1 mL syringe. For each reaction time point, the time since

DnaK and ATP* had been mixed was noted to permit correction for ATP hydrolysis that had occurred in the syringe prior to the addition of DnaJ (see below).

Analysis of Data. Data points corresponding to the fraction of input ATP hydrolyzed at a given time ($fracADP_t$) were normalized using eq 1 for the fraction of the starting material present as ADP ($fracADP_0$, typically 0.01−0.03), and for the fraction of unreactive material (represented as $fracATP^*_\infty$; typically ∼0.05) that remains at the origin in the thin-layer chromatographic analysis. This unreactive material has little or no affinity for DnaK (data not shown).

$$\mathrm{fracADP_{norm}} = \frac{\mathrm{fracADP}_t - \mathrm{fracADP}_0}{(1 - \mathrm{fracATP^*}_\infty) - \mathrm{fracADP}_0} \quad (1)$$

Data from those rapid-quench experiments initiated by mixing DnaK·ATP* with DnaJ were further corrected for hydrolysis that occurred in the syringe prior to the addition of DnaJ. For each reaction time point, the expected amount of hydrolysis was calculated based on the amount of time since ATP* and DnaK had been mixed and on the calculated rate constant for intrinsic hydrolysis by DnaK at room temperature[2] (*22*). Rates of intrinsic hydrolysis were verified at the completion of each time course (typically 25−30 min) by measuring the fraction of ADP* in an aliquot of the DnaK·ATP* mix that had not been mixed with DnaJ. This was generally within 5% of the expected value (∼35−40% ADP*). The data from each time point were then corrected for intrinsic hydrolysis using eq 2, where $fracADP_{exp}$ is the calculated fraction of nucleotide present as ADP* at the time the reaction was initiated with DnaJ.

$$\mathrm{fracADP_{corrected}} = \frac{\mathrm{fracADP_{norm}} - \mathrm{fracADP_{exp}}}{1 - \mathrm{fracADP_{exp}}} \quad (2)$$

Progress curves of ATP hydrolysis ($fracADP_{norm}$ or $fracADP_{corrected}$) were fitted using Enzfitter to an equation describing first-order kinetics (eq 3), or in cases where a lag was visible, to an equation including two consecutive steps (eq 4), where in both cases t is time and $fracADP_{end}$ represents the reaction end point.

$$\mathrm{fracADP_{norm}} = \mathrm{fracADP_{end}}(1 - e^{-k_{obs}t}) \quad (3)$$

$$\mathrm{fracADP_{norm}} = \mathrm{fracADP_{end}}\left(1 + \frac{\lambda_2 e^{-\lambda_1 t} - \lambda_1 e^{-\lambda_2 t}}{\lambda_1 - \lambda_2}\right) \quad (4)$$

Data from multiple-turnover ATPase experiments were fitted to eq 4, which was modified to include an additional term representing steady-state hydrolysis. In this case, $fracADP_{end}$ represents the amount of ATP hydrolyzed in the rapid initial phase.

Analysis of Error. Results are reported plus or minus one standard deviation from the curve fitting. It was generally found that random deviation within an experiment was less than that between experiments; the latter generally did not exceed 20−30%.

RESULTS

Multiple-Turnover ATPase Activity of DnaK. It has previously been shown that DnaJ is capable of stimulating the single-turnover ATPase activity of DnaK ≥200-fold (*27*). However, substantial stimulation in the steady state requires the simultaneous presence of GrpE (*21*, *23*, *26*); presumably this is because product release (ADP or P_i) becomes rate-limiting, and DnaJ does not stimulate these steps. To confirm this, we performed ATPase experiments under multiple-turnover conditions, with ATP* present in 5-fold molar excess over DnaK. The time scale of these experiments necessitated the use of a rapid quench-flow apparatus (see Materials and Methods). We found that a fraction of the ATP* was hydrolyzed quickly (within 30 s, Figure 1); this fraction corresponded to 1.0 ± 0.1 mol of ATP/DnaK. This stoichiometry was unaffected by changes in ATP concentration (data not shown). The steady-state rate of hydrolysis following this initial turnover was 0.24 ± 0.02 mol of ATP·(mol of DnaK)$^{-1}$·min^{-1}, similar to the rate constant for ADP release from DnaK [0.4 min^{-1} in the absence of inorganic phosphate (*22*)]. The results are thus consistent with a model in which ADP release is rate-limiting in the steady state in the presence of DnaJ. As expected, inclusion of GrpE in the reaction did not affect the initial rate of hydrolysis. It did, however, eliminate the plateau; hydrolysis proceeded rapidly to completion, with a steady-state rate constant of approximately 5−6 min^{-1}.[3] This is consistent with previously reported steady-state rates under similar conditions (*21*).

Closer inspection of the early part of the progress curve in the presence of DnaJ revealed that it is composed of two phases, with a pronounced kinetic lag (Figure 1, inset). A fit of the data to a modified eq 4 (see Materials and Methods) yielded observed rate constants of 51 ± 12 and 10.8 ± 1.0 min^{-1} (λ_1 and λ_2). These observed rate constants represent microscopic rate constants only if there are exactly two kinetically significant steps in the process leading to ADP production, both of which are irreversible (*49*). In this case, it is likely that there are at least three steps which may be kinetically significant (Figure 2). ATP binding to Hsc70 and DnaK has been shown to involve at least two steps, including a first-order isomerization step following initial encounter (*20*, *50*). DnaJ association with DnaK·ATP is apparently a rapid equilibrium step with respect to the chemical step (see below), so a third step which may be kinetically significant is hydrolysis of nucleotide.

To establish whether diffusion-limited binding of ATP (k_1) is kinetically significant, similar multiple-turnover experiments were performed using higher concentrations of ATP. These increases had little effect on λ_2 (11.4 ± 1.0 and 14.4 ± 7.3 min^{-1} at 10 and 20 μM ATP, respectively). There

[2] The calculation of the intrinsic hydrolysis rate was made at room temperature because the sample syringes on the rapid quench instrument are located outside the thermostated region. Each sample aliquot was equilibrated to 25 °C for a time equivalent to one reaction cycle (∼2 min) prior to injection. No correction was made for the increased intrinsic hydrolysis during this time relative to that at room temperature.

[3] Calculation of an initial steady-state rate requires that product inhibition not be significant; thus, reactions are typically followed only to 5−10% conversion to product. Under the conditions of this experiment, the presence of a kinetic lag precluded the use of this portion for steady-state rate calculations. The time course of hydrolysis is essentially linear to 50−60% ADP, and control experiments have shown that GrpE virtually eliminates product inhibition in the absence of DnaJ under similar conditions. Thus, product inhibition is unlikely to significantly affect calculation of this rate.

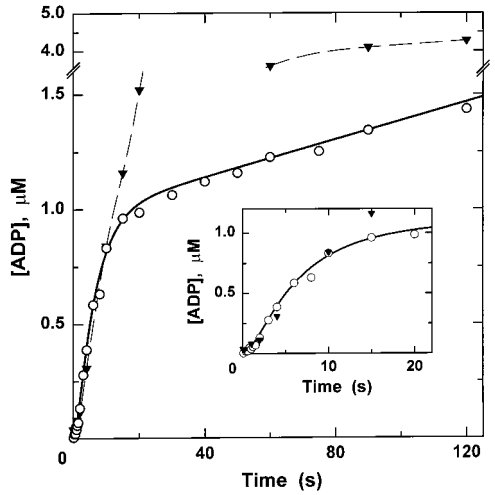

FIGURE 1: Multiple-turnover ATPase activity of DnaK in the presence of DnaJ. Reaction mixtures contained 1 μM DnaK, 5 μM ATP*, and 2 μM DnaJ (○), or 2 μM DnaJ and 2 μM GrpE (▼). The reactions were performed in HM buffer using a rapid-quench apparatus as described under Materials and Methods. In the presence of DnaJ and absence of GrpE, a burst of ADP* is produced that is stoichiometric with DnaK. This initial phase of hydrolysis includes a kinetic lag (inset; circles). Including GrpE in the reaction mixture did not significantly affect the lag (inset; triangles) or the initial phase of hydrolysis, but did cause hydrolysis to proceed rapidly to completion. The dashed line is shown only to guide the eye.

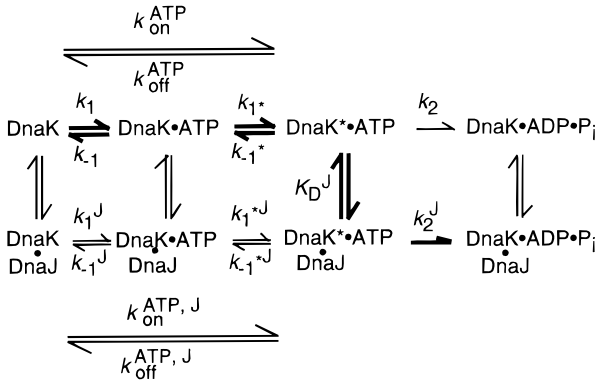

FIGURE 2: Kinetic scheme for ATP hydrolysis by DnaK in the presence of DnaJ. The boldface arrows indicate the kinetic pathway of greatest flux leading to hydrolysis under the conditions of these experiments [excess DnaJ (0.5−20 μM) over DnaK], for reasons described in the text. Rate constants are labeled for the intrinsic reaction of DnaK as described previously (*22*), except that ATP binding is shown as two steps, following the nomenclature established for eukaryotic Hsc70 (*50*). The kinetic constants above and below the scheme, accompanying the long arrows, represent experimentally determined values for rates of binding and release of ATP, and are composites of microscopic rate constants. Hydrolysis steps (k_2 and k_2^J) are shown as being irreversible because we and others have been unable to detect net synthesis of ATP from ADP and P_i (*17*, *20*, *22*) in the presence or absence of DnaJ (data not shown). Following ATP hydrolysis, DnaK is no longer shown as "DnaK*" because it is likely that there is a conformational change associated with hydrolysis of nucleotide (*20*). This is not meant to imply that DnaK necessarily reverts to its original conformation at this step. The constants k_1 and k_1^J are second-order rate constants for binding of ATP, and K_D^J represents the equilibrium dissociation constant for DnaJ and DnaK·ATP. Free ATP and free DnaJ are not shown explicitly.

was not a dramatic effect on λ_1 either; however, quantitation became unreliable as the fraction of ATP* associated with the initial phase decreased to 5% of the total at 20 μM ATP. Increasing the concentration of DnaJ 2.5-fold also had little or no effect on λ_1 or λ_2 (data not shown). Taken together, the results suggest that there are at least two kinetically significant first-order events on the pathway to ATP hydrolysis and indicate that DnaJ stimulates the rate of hydrolysis at least 500-fold ($k_2^J \geq 11$ min^{-1}). This experiment only sets a minimum for the DnaK ATP hydrolysis rate in the presence of DnaJ, since it is not clear which observed rate constant, if either, represents the hydrolysis step specifically. Subsequent experiments, described below, suggest that λ_2 represents a conformational change of DnaK elicited by ATP binding and that λ_1 is associated with ATP hydrolysis.

Effects of DnaJ on ATP Binding and Release by DnaK. We have previously shown that in the absence of DnaJ, ATP release is slightly slower than hydrolysis ($k_2 = 0.02$ min^{-1}; $k_{off}^{ATP} = 0.008$ min^{-1}),[4] such that approximately 75% of ATP bound by DnaK is hydrolyzed rather than being released (*22*). To further delineate the pathway of greatest flux leading to hydrolysis (Figure 2), we examined the partitioning of bound ATP in the presence of DnaJ. Limiting ATP* was preincubated with DnaK to allow for binding, followed by the simultaneous addition of DnaJ and a vast excess of unlabeled ATP. The partitioning of ATP* was monitored by following the hydrolysis reaction to a plateau, which was determined to be essentially 100% conversion to ADP* (data not shown), demonstrating that $k_2^J \gg k_{off}^{ATP,J}$. This partitioning was independent of moderate changes in the DnaJ concentration, as expected since both k_2 and k_{off}^{ATP} are much slower than k_2^J. This experiment, however, does not rule out an effect of DnaJ on the ATP release rate, since a substantial increase would be difficult to detect due to the large increase in the hydrolysis rate. Assuming a detection limit of 1−2% ADP at the plateau, the stimulation of hydrolysis must be at least 20-fold greater than any stimulation of ATP release. While it does not rule out an effect of DnaJ on ATP release, this result demonstrates that when the DnaK·ATP complex encounters DnaJ, ATP is rarely released from DnaK; it is either hydrolyzed or DnaK·ATP dissociates from DnaJ before ATP is hydrolyzed or released.

The finding that hydrolysis of bound ATP is much faster than release when DnaJ is present leads to the prediction that at subsaturating DnaK concentrations a single turnover should be limited by the binding of ATP (i.e., $k_{cat}/K_M = k_{on}^{ATP}$). This was verified experimentally by comparing observed rates of ATP binding and hydrolysis at subsaturating concentrations of DnaK. DnaK and DnaJ were preincubated, and reactions were initiated with limiting ATP*. Aliquots were quenched with HCl to measure hydrolysis, or excess unlabeled ATP to measure binding (*48*). As shown in Figure 3A, at a given concentration of DnaK, the disappearance of unbound ATP* (circles; $k_{obs} = 1.4$ min^{-1}) is closely matched with the appearance of ADP* (triangles; $\lambda_2 = 1.5$ min^{-1}). A kinetic lag was reproducibly visible in the reactions monitoring hydrolysis. The observed rate constant of the lag (λ_1) was essentially independent of [DnaK], but increased with [DnaJ] between 0.2 and 2 μM (data not shown), suggesting that the lag reflects a process

[4] This previous analysis was performed assuming single-step binding and release. With the additional step included, the observed rate constant is a composite of the two steps, or $k_{off}^{ATP} \approx k_{-1}^* k_{-1}/(k_1^* + k_{-1})$.

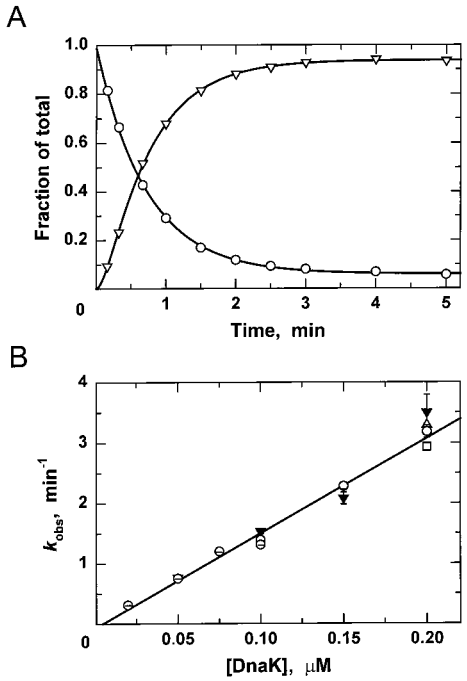

FIGURE 3: Comparison of ATP binding and hydrolysis rates at low [DnaK]. (A) At 0.1 μM DnaK and 0.5 μM DnaJ, the disappearance of unbound ATP* (○) is matched by the appearance of ADP* (▽). Reactions were performed using limiting ATP*, and time points were quenched with excess unlabeled ATP, to monitor binding, or with HCl, to monitor hydrolysis (see Materials and Methods). Equation 2 was fitted to the binding data, yielding a pseudo-first-order rate constant of 1.39 ± 0.02 min^{-1}. Equation 3 was fitted to the hydrolysis data, which includes a kinetic lag, yielding observed rate constants of 7.0 ± 0.5 and 1.53 ± 0.04 min^{-1}. The smaller of the two rate constants reflects rate-limiting binding of ATP, while the larger represents an additional step(s), as described in the text. (B) Plot of observed ATP binding (○) and hydrolysis (▼) rate constants as a function of DnaK concentration. Reactions were performed as in (A), using 0.5 μM DnaJ. The observed pseudo-first-order rate constant for ATP binding was found to vary linearly with [DnaK], yielding a second-order rate constant of 1.5×10^7 M^{-1} min^{-1}. At 0.2 μM DnaK, lowering [DnaJ] to 0.2 μM (□) or raising it to 2 μM (△) had negligible effect on the observed rate of ATP binding.

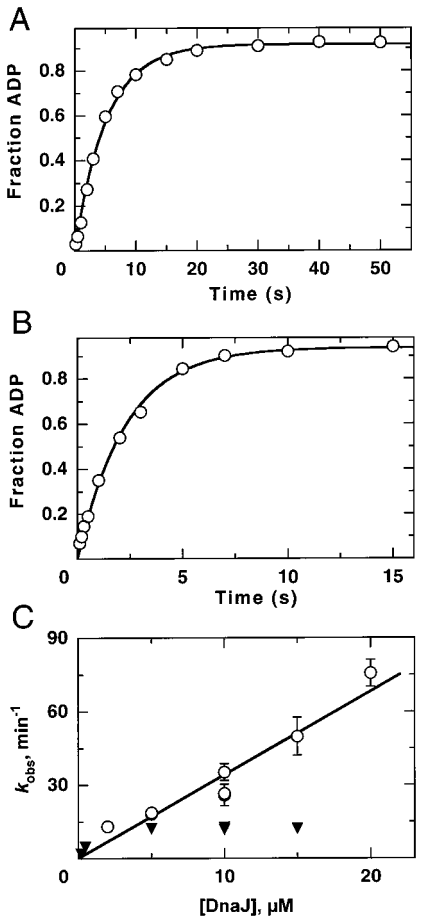

FIGURE 4: Single-turnover ATPase activity of DnaK in the presence of DnaJ at 25 °C. (A) DnaK (5 μM) and DnaJ (10 μM) were preincubated together, and reactions were subsequently initiated with limiting ATP* using a rapid-quench apparatus (see Materials and Methods). A first-order rate equation (eq 3) was fitted to the data, yielding $k_{obs} = 11.7 \pm 0.4$ min^{-1}. (B) Limiting ATP* was added to DnaK (1 μM), and reactions were subsequently initiated with the addition of DnaJ (10 μM) using a rapid-quench apparatus. Individual time points were corrected for the amount of ATP hydrolysis that had occurred prior to the addition of DnaJ (see Materials and Methods). Equation 3 was fitted to the data, yielding $k_{obs} = 26.4 \pm 1.2$ min^{-1}. (C) Comparison of observed rate constants from reactions initiated with ATP (▼) or DnaJ (○) as a function of DnaJ concentration. Results were plotted from reactions performed as described in (A) or (B).

associated with ATP hydrolysis rather than ATP binding. Plots of observed rates of binding and observed rates of hydrolysis as a function of [DnaK] are superimposable (Figure 3B), demonstrating that under these conditions $k_{cat}/K_M = k_{on}$, as predicted from the partitioning experiment. Furthermore, the slope of the line yields a value for k_{on}^{ATP} of 1.5×10^7 M^{-1} min^{-1}, very similar to the value of 8.0×10^6 M^{-1} min^{-1} measured in the absence of DnaJ (*22*). Thus, at the concentration of DnaJ used in these experiments (0.5 μM), there is minimal effect of DnaJ on the rate of ATP binding. Variation of DnaJ concentration across a 10-fold range produced only a 10% increase in the observed rate of ATP binding (Figure 3B), a further indication that DnaJ does not dramatically affect this rate or is not bound to DnaK at these concentrations.

Detection of a Change in the Rate-Limiting Step for Single-Turnover ATPase Activity. To determine the maximal amount of ATPase stimulation by DnaJ, single-turnover experiments were performed as a function of [DnaJ]. DnaJ was preincubated with DnaK, and reactions were initiated with the addition of limiting ATP*. At low [DnaJ] (≤ 5 μM), progress curves were composed of two phases, including a kinetic lag; at higher DnaJ concentrations, the lag was poorly resolved, and the progress curves were reasonably well described by a single rate constant ($k_{obs} = 11.7 \pm 0.4$ min^{-1} at 10 μM DnaJ; Figure 4A). Increasing the concentration of DnaJ above 5 μM did not result in a further increase in k_{obs} (Figure 4C, triangles). Rather, the reaction rate constant appeared to plateau at $\sim$11−13 min^{-1}, very similar to the maximal rate constant observed previously in multiple-turnover reactions. As observed under multiple-turnover conditions, this plateau was not due to second-order binding of ATP becoming rate-limiting, since increasing the concentration of DnaK had no effect on k_{obs} (data not shown).

Though second-order binding of ATP was not rate-limiting, it remained possible that a first-order step prior to ATP hydrolysis becomes rate-limiting at high [DnaJ]. Since it is likely that at least one conformational change of DnaK accompanies ATP binding (*18*, *20*), this first-order conformational change represents an additional step which could

be rate-limiting. To address this possibility, we performed an analogous series of reactions in which DnaK was first preincubated with limiting ATP*, and rapid ATP hydrolysis was subsequently initiated by the addition of DnaJ. With this experimental protocol, if the rate-limiting step was associated with ATP binding, it would not contribute to k_{obs}, since the ATP binding step would already have occurred during the preincubation.

When single-turnover ATPase reactions were initiated with DnaJ, progress curves were first-order at all DnaJ concentrations tested (2−20 μM), and at high [DnaJ] reactions were significantly faster than were analogous reactions initiated with ATP. For example, at 10 μM DnaJ, k_{obs} was 26.4 ± 1.2 min^{-1} (Figure 4B, compare with Figure 4A). No hint of a plateau was observed, as k_{obs} rose linearly with [DnaJ] to ≥20 μM with a slope of ∼3.3 × 10^6 M^{-1} min^{-1} (Figure 4C). At the highest concentration of DnaJ tested (20 μM), k_{obs} was 75.7 ± 5.6 min^{-1}, indicating that the maximal stimulation of hydrolysis by DnaJ is greater than ∼4000-fold. We have previously shown that the concentration of DnaK used in these experiments (2 μM in the preincubation with ATP*) is saturating for binding of ATP (*22*); not surprisingly, variation of [DnaK] from 0.5 to 2 μM had no effect on k_{obs} (data not shown).

Determination of Maximal Stimulation by DnaJ at 5 °C. In an attempt to more precisely delimit the maximal extent of DnaJ-mediated stimulation of ATP hydrolysis by DnaK, we examined the impact of DnaJ on the DnaK ATPase at 5 °C, performing assays similar to those described in the preceding section. At this lower temperature, reactions were sufficiently slow that they could be performed by hand, in smaller volumes, which both permitted a simplified kinetic analysis and helped conserve reagents.

Reactions were performed, as at 25 °C, either by initiating with ATP* or by adding DnaJ to a preformed DnaK·ATP* complex (Figure 5A). Qualitatively, the results were similar to those obtained at 25 °C. Reactions were first-order,[5] and at low concentrations of DnaJ (≤2 μM), k_{obs} was independent of the nature of the initiator (ATP* or DnaJ). However, at higher [DnaJ], a striking divergence was observed. Reactions initiated with ATP* proceeded no faster than ∼1 min^{-1}. In contrast, k_{obs} for those reactions initiated with DnaJ followed a hyperbolic dependence on DnaJ, yielding values of 18.7 ± 1.6 μM for K_A and 15.2 ± 0.8 min^{-1} for k_{cat} (Table 1). The parameter k_{cat} represents the maximal ATPase rate in the presence of DnaJ (k_2^J); the physical relevance of the K_A term is discussed below. The intrinsic ATPase rate of DnaK at 5 °C was determined to be 9.9 × 10^{-4} min^{-1} (data not shown; Table 1); therefore, DnaJ accelerates the ATP hydrolysis rate ∼15 000-fold at 5 °C.

During the course of these experiments it was observed that replacement of potassium glutamate (K^+Glu^-) with KCl had a significant effect on the observed hydrolysis rate at 5 °C in the presence of DnaJ. To further investigate this effect, we performed ATPase reactions in KCl as a function of [DnaJ], again initiating reactions with the addition of DnaJ or ATP* (Figure 5B). When initiation was with DnaJ, the dependence of k_{obs} on [DnaJ] was again hyperbolic, yielding values for K_A and k_{cat} of 18.5 ± 4.5 μM and 1.2 ± 0.2 min^{-1}, respectively. Thus, there is little or no effect of replacing Glu^- with Cl^- on K_A; however, k_2^J is reduced ∼13-fold. This difference is specific to the presence of DnaJ, as the

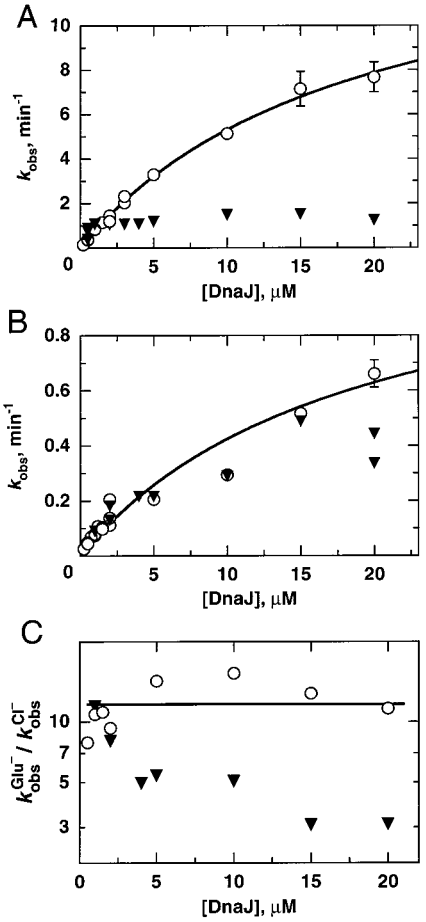

FIGURE 5: Single-turnover ATPase activity of DnaK in the presence of DnaJ at 5 °C, and effect of anion. (A) Reactions were performed in HM buffer, containing 200 mM K^+Glu^-, and were initiated with the addition of DnaJ (○) or ATP* (▼). In all cases [DnaK] was 1 μM, ATP* was limiting, and reactions were sufficiently slow that they could be monitored by hand. (B) Reactions were performed as described for (A), except that K^+Glu^- was replaced with 200 mM KCl. Note that the ordinates of (A) and (B) differ by >10-fold. (C) To illustrate the effect of anion, observed rate constants from (A) for reactions initiated with DnaJ (○) or ATP (▼) were divided by those from (B).

Table 1: Summary of Rate and Equilibrium Constants[a]

	25 °C	5 °C
k_{on}^{ATP} (M^{-1} min^{-1})	8.0 × 10^6 [b]	ND[c]
k_{off}^{ATP} (min^{-1})	0.008[b]	ND
k_2 (min^{-1})	0.018[b]	0.00099
k_1^* (min^{-1})	14	1.5
K_D^J (μM)	>20	20
k_2^J (min^{-1})	∼300[d]	15
$k_{off}^{ATP,J}$	<3	ND

[a] Obtained in 50 mM Hepes/KOH, pH 7.6, 11 mM magnesium acetate, and 200 mM potassium glutamate. [b] Data from ref *22*. [c] ND, not determined. [d] This value is calculated from the rate constant for ATP hydrolysis for DnaK at 25 °C, k_2, and from the 15 000-fold stimulation of ATP hydrolysis provided by saturating levels of DnaJ at 5 °C (see text).

[5] In some experiments at 5 °C, a poorly resolved kinetic lag was visible. However, its presence was irreproducible, and in cases where it was present there was no detectable dependence on the concentration of DnaJ. Furthermore, it was not observed at 25 °C using rapid-quench techniques. Therefore, it is most likely an artifact of manual mixing.

intrinsic ATPase rate of DnaK at 5 °C in the presence of Cl^- was determined to be identical to that measured in Glu^- (data not shown). At 25 °C, the effect of Cl^- on k_2^J was present, but less dramatic (~4-fold; data not shown).

What Does K_A Represent? At 5 °C, a hyperbolic dependence of the observed rate constant for hydrolysis on [DnaJ] was observed when reactions were initiated with DnaJ. The resulting fits yielded values for K_A of ~20 μM in the presence of both Glu^- and Cl^-. In general, K_A, like K_M, can be a complex parameter containing terms representing both binding of substrate and first-order steps on the reaction pathway (*48*). In this perspective, the activating cochaperone, DnaJ, is considered to be the "enzyme", DnaK·ATP is the "substrate", and reactions are single turnover, with DnaJ "enzyme" in excess. The argument outlined below suggests that initial binding of DnaJ to DnaK·ATP is in rapid equilibrium with respect to hydrolysis of ATP, and, thus, K_A represents K_D^J, the equilibrium dissociation constant for DnaJ binding to DnaK·ATP.

The observation that progress curves were first-order indicates that there is only one kinetically significant step leading to hydrolysis under these conditions. At least two events must occur (eq 5): DnaJ binds DnaK·ATP, and ATP is hydrolyzed.

$$\text{DnaJ} + \text{DnaK·ATP} \underset{k_{off}^J}{\overset{k_{on}^J}{\rightleftharpoons}} \text{DnaJ·DnaK·ATP} \xrightarrow{k_2^J} \text{DnaJ·DnaK·ADP·P}_i \quad (5)$$

Additionally, there may be one or more conformational changes associated with DnaJ binding or leading to ATP hydrolysis; however, this is the simplest mechanism that accounts for the data. In general, given the mechanism in eq 5, k_{obs} will be dependent on the concentration of DnaJ in the manner shown in eq 6.

$$k_{obs} \approx \frac{k_{on}^J[\text{DnaJ}]k_2^J}{k_{on}^J[\text{DnaJ}] + k_{off}^J + k_2^J} \quad (6)$$

Since there is only one kinetically significant step on the pathway, k_{off}^J must be substantially different from k_2^J (either much greater than k_2^J or much less than k_2^J). This leads to two possible explanations for the dependence of k_{obs} on [DnaJ]. (1) Binding of DnaJ, a second-order process, is rate-limiting at low [DnaJ]. This requires that DnaJ binding is essentially irreversible ($k_{off}^J \ll k_2^J$), and in this case eq 6 reduces to $k_{obs} \approx k_2^J[\text{DnaJ}]/([\text{DnaJ}] + (k_2^J/k_{on}^J))$. This is directly analogous to the Michaelis−Menten equation, in which $k_{cat} = k_2^J$ and $K_M = K_A = k_2^J/k_{on}^J$. In this scenario, the limiting slope of the hyperbola at low [DnaJ] is the second-order rate constant k_{on}^J. (2) Binding of DnaJ is in rapid equilibrium ($k_{off}^J \gg k_2^J$), and hydrolysis or a first-order process leading to hydrolysis is rate-limiting. Equation 6 reduces to $k_{obs} \approx k_2^J[\text{DnaJ}]/([\text{DnaJ}] + K_D^J)$, where $K_D^J = k_{off}^J/k_{on}^J$. Under these conditions, the limiting slope of the line at low DnaJ concentration, i.e., the apparent second-order rate constant, is equal to k_2^J/K_D^J.

We consider rate-limiting binding (case 1) unlikely for three reasons. First, the determined slope at low [DnaJ] (3.3×10^6 M^{-1} min^{-1} at 25 °C; 8.1×10^5 M^{-1} min^{-1} at 5 °C) is nearly 5 orders of magnitude below the diffusion-limited association rate of two similarly sized molecules (*51*), and is thus unlikely to represent k_{on}^J. Furthermore, the apparent second-order rate constant is 4-fold higher at 25 °C than at 5 °C. The true second-order rate constant for association would be expected to vary proportionally with temperature (in kelvin), and would be nearly unchanged between 5 and 25 °C. Nonetheless, however improbable, both of these observations could potentially be explained by a model in which rate-limiting binding is preceded by an unfavorable conformational change in DnaJ that is required for binding. This would lower the concentration of active DnaJ, explaining the very low apparent second-order rate constant, and the temperature dependence could be explained by an effect on the equilibrium of the conformational change.

The third reason rate-limiting binding of DnaJ is unlikely is related to the effect of replacing glutamate anion with chloride anion. This replacement was observed to decrease the plateau of k_{obs} ~13-fold at 5 °C; in either case, the plateau represents k_2^J. The limiting slope at low [DnaJ], k_{cat}/K_A, was observed to decrease by a similar amount (Figure 5B). In a model invoking rate-limiting binding of DnaJ, $k_{cat}/K_A = k_{on}^J$ and, in contrast to our results, k_{cat}/K_A should have remained constant. The observed decrease in k_{cat}/K_A requires that k_{on}^J was fortuitously decreased by a similar amount as k_2^J. Even with the assumption of a prior conformational change in DnaJ, a fortuitous change in the equilibrium constant for the rearrangement is required to explain the change in k_{cat}/K_A. In contrast, a rapid-equilibrium model (i.e., explanation 2) predicts that $k_{cat}/K_A = k_2^J/K_D^J$, and so a change in k_2^J would result in a similar change in k_{cat}/K_A. For these reasons, we favor a model in which binding of DnaJ to DnaK·ATP is in rapid equilibrium with respect to ATP hydrolysis, and therefore $K_A = K_D^J$ (~20 μM at 5 °C).

Effect of Cl^- on the Change in Rate-Limiting Step. In the presence of Glu^- at 5 °C, there was a striking divergence of k_{obs} as a function of [DnaJ] depending on whether reactions were initiated with the addition of DnaJ or ATP* (Figure 5A). This was postulated to represent a change in the rate-limiting step in the case of reactions initiated with ATP*, to a first-order step of ~1 min^{-1} at 5 °C that is associated with ATP binding (since the step apparently proceeds essentially to completion when ATP* is mixed with DnaK prior to the addition of DnaJ). This first-order step is therefore assigned as k_1^* and represents the conformational change that occurs upon ATP binding (Figure 2). Replacement of Glu^- with Cl^- leads to a 13-fold decrease in k_2^J, so even at high DnaJ concentrations, k_{obs} for reactions initiated with DnaJ is <1 min^{-1} (Figure 5B). We therefore predicted that in the presence of Cl^-, k_2^J would remain rate-limiting in reactions initiated with ATP*, even at DnaJ concentrations significantly higher than 2 μM, which was the point of rate divergence in the presence of Glu^- (Figure 5A). This prediction was borne out experimentally to DnaJ concentrations as high as 15 μM, since, in the presence of Cl^-, the plots of k_{obs} as a function of [DnaJ] indicate that the nature of the initiator has little or no effect on the observed ATPase rate (Figure 5B). At 15−20 μM DnaJ, however, k_{obs} may be significantly lower when the reaction is initiated with ATP. This suggests that Cl^- could have a minor effect on k_1^*, decreasing it from ~1 to ~0.4 min^{-1} at 5 °C.

Because replacing Glu^- with Cl^- has a much larger effect on k_2^J than on k_1^*, a comparison of k_{obs} in the presence of glutamate anion versus that in chloride anion, i.e., $k_{obs}^{Glu}/k_{obs}^{Cl}$, may be generally useful as a method for determining whether k_2^J is rate-limiting under a given set of conditions. In reactions initiated with DnaJ, $k_{obs}^{Glu}/k_{obs}^{Cl}$ is essentially constant across the range of DnaJ concentrations tested, consistent with the idea that k_2^J remains rate-limiting (Figure 5C). In contrast, for reactions initiated with ATP*, $k_{obs}^{Glu}/k_{obs}^{Cl}$, is dependent on the concentration of DnaJ, decreasing from ~10 at low [DnaJ] to ~3 at 15 μM DnaJ. Thus, as the concentration of DnaJ is increased under these conditions, there is a change in the rate-limiting step to one (k_1^*) which is less affected by the nature of the anion.

DISCUSSION

A Kinetic Model for ATP Hydrolysis by DnaK in the Presence of DnaJ. By measuring the ATPase rate of DnaK under single-turnover conditions in the presence of various concentrations of DnaJ, we have determined (Table 1) approximate values at 5 °C for the first-order rate constant for hydrolysis of ATP from the DnaJ·DnaK·ATP complex ($k_2^J \approx 15\ min^{-1}$) and have defined the equilibrium dissociation constant for the complex formed between DnaJ and DnaK·ATP ($K_D^J \approx 20\ \mu M$). Additionally, we have found that at sufficient concentrations of DnaJ, ATP binding is rate-limiting for hydrolysis when ATP is added to a reaction containing DnaK and DnaJ.

These results have been interpreted in the context of Figure 2 (see also Table 1), where the boldface arrows indicate the predominant pathway under these experimental conditions. ATP binding to DnaK proceeds in at least two steps (*20*, *52*). It is not clear whether DnaJ associates with DnaK prior to ATP binding by DnaK; however, because the concentrations of DnaJ in most experiments were substantially lower than K_D^J and no significant effects of DnaJ on the kinetics of ATP binding to DnaK have been detected, the simplest model involves ATP binding primarily to free DnaK. In any case, DnaJ association with DnaK·ATP appears to be in rapid equilibrium with respect to ATP hydrolysis (i.e., $k_{off}^J \gg k_2^J$), so even if DnaJ is associated with DnaK prior to ATP binding, it is likely to dissociate before ATP is hydrolyzed. No evidence was obtained in partitioning experiments for any significant flux through the lower pathway in the reverse direction leading to the dissociation of ATP from the DnaJ·DnaK complex (i.e., $k_{off}^{ATP,J} \ll k_2^J$). Thus, all the experiments described are consistent with a model in which nearly all hydrolytic events result from DnaJ associating with a preformed DnaK·ATP complex, which partitions exclusively toward hydrolysis. This general model is consistent with proposals that DnaJ functions as a specificity factor to target polypeptide substrates to DnaK, as discussed in more detail below (see *A Kinetic Model for DnaJ-Mediated Specificity*).

Rate-Limiting ATP Binding. As the concentration of DnaJ is increased, ATP binding by DnaK becomes rate-limiting for hydrolysis (Figures 3B, 4, and 5). At low concentrations of DnaK (<1 μM), a linear dependence of k_{obs} on [DnaK] exists, but at higher DnaK concentrations, the dependence is lost, consistent with a multistep binding pathway, as previously described for both DnaK (*20*, *52*) and eukaryotic Hsc70 (*50*). The plateau of k_{obs} thus measures a first-order step that follows the initial encounter, and is ~12−15 min^{-1} at 25 °C (Figure 4C). It is likely that this represents the slow first-order step previously identified in kinetic studies of ATP binding to DnaK (*20*, *53*). Slepenkov and Witt (*52*) have reported a rate constant of 40 ± 12 min^{-1}, only slightly larger than measured here. The small difference may be due to the presence of DnaJ in our experimental system, or to differences in buffer conditions or K^+ concentration. Theysson et al. (*20*) reported a somewhat higher rate constant of 90 min^{-1}. However, they reported that peptides accelerate this step significantly; moreover, it has been inferred (*22*) that the DnaK preparations used in those studies may have contained small amounts of endogenous peptides, which, if so, could explain the higher rate. Taken together, the available evidence suggests that DnaK undergoes a slow isomerization upon binding ATP, an isomerization that is rate-limiting for hydrolysis when sufficient DnaJ is present.

Is ATP Binding Rate-Limiting for ATP Hydrolysis in Vivo? It is generally thought that a pool of DnaK·ATP exists in vivo, and that the chaperone action of DnaK results from the binding of this DnaK form to a polypeptide substrate (in the presence or absence of DnaJ). This is akin to in vitro experiments where hydrolysis is initiated with the addition of DnaJ, a condition where the isomerization of DnaK associated with ATP binding is not rate-limiting. However, it is possible that for some functions of DnaK, multiple cycles of polypeptide binding and release (and hence ATPase cycles) are required. This can be imagined, for example, for protection of heat-denatured proteins from aggregation or for the process of protein folding. DnaK·ATP binds unfolded or partially folded nascent polypeptides, and subsequent ATP hydrolysis produces the ADP form of DnaK that binds polypeptides most tightly, thereby interfering with protein aggregation [reviewed in (*6*, *7*)]. With some frequency, the polypeptide is released by DnaK, providing a fresh opportunity to fold or to interact with other chaperones or chaperonins (such as with GroEL, a member of the ubiquitous cpn60 family). Alternatively, the released polypeptide may rebind to DnaK. The available evidence indicates that DnaJ and GrpE play central roles in facilitating multiple ATPase cycles. It is certainly conceivable that the rates of both ATP hydrolysis and ADP release are increased by the action of these cochaperones to ≫15 min^{-1}, such that k_1^* could become rate-limiting for the overall cycle in vivo. Consistent with this notion, the maximal steady-state ATPase rates reported in the presence of both DnaJ and GrpE are in this range [(*21*); A. W. Karzai and R. McMacken, unpublished results]. The capacity of peptide to stimulate k_1^* (*20*) may be key, since our data indicate that, under optimal conditions, this step becomes the slowest step in the DnaK ATPase cycle.

Magnitude of the ATPase Rate Enhancement by DnaJ. The maximal stimulation of the ATPase rate of DnaK was determined to be ~15 000-fold at 5 °C. At 25 °C, the dependence of k_{obs} on [DnaJ] was linear to the highest concentration of DnaJ used; thus, a direct measurement of the maximal stimulation was not made. It is notable, however, that an Arrhenius plot of the intrinsic ATPase rate constant for DnaK is linear from 5 to 40 °C [(*22*) and this work]. Furthermore, measurement of the ATPase rate in the

presence of a fixed (nonsaturating) concentration of DnaJ produced a linear Arrhenius plot from 5 to 15 °C, with an activation energy similar to that for the intrinsic reaction (R. Russell and R. McMacken, unpublished results). It is therefore unlikely that the maximal stimulation by DnaJ at 25 °C is dramatically different from that measured at 5 °C. However, since the affinity of DnaJ for DnaK·ATP appears to decrease marginally with increasing temperature, the temperature dependence, and hence the maximal stimulation at 25 °C, may be slightly underestimated.

We have previously shown that in the presence of physiologically relevant concentrations of P_i (5−10 mM) the intrinsic rates of ATP hydrolysis and ADP release by DnaK are essentially equal at 25 °C (both are ∼0.02 min^{-1}) (*22*). A recent report from Slepenkov and Witt (*52*) is in general agreement with this finding. They determined that the rate of ADP release is within 3−5-fold of the rate of ATP hydrolysis in the presence of P_i over the 25−35 °C temperature range. It is interesting that the approximate balance in ATP hydrolysis and ADP release rates is still maintained during maximum stimulation of DnaK by its cochaperone activators. A recent study has determined the maximum stimulation of ADP release by GrpE to be ∼5000-fold (*28*), quite similar to the maximal stimulation of ATP hydrolysis we have observed for DnaJ.

Because ATP hydrolysis and ADP release are by far the slowest steps in the intrinsic ATPase cycle of DnaK, the protein partitions between ATP- and ADP-bound forms in the steady-state (where the ADP-bound form may also contain bound P_i, depending on the concentration of inorganic phosphate). Furthermore, in the absence of cochaperones, it is the ratio between the rate constants corresponding to these two steps that under a given set of conditions determines the ratio of ATP- and ADP-bound DnaK forms (*22*). The properties of these two forms differ substantially in their polypeptide binding properties. The ATP-bound form is characterized by weak binding to polypeptides [K_D in the micromolar range (*18*, *20*)], while the ADP-bound form binds polypeptides much more stably (*54*). In vivo, it may be necessary to maintain or, at times, rapidly create a reservoir of ATP-bound DnaK that is primed to act on target polypeptides. This may be especially important under conditions where there exists a significant population of ADP·DnaK tightly associated with polypeptides. Regulation of the concentrations and lifetimes of these two states may be critical to optimal cellular protein metabolism. Action of the DnaJ and GrpE cochaperones to stimulate ATP hydrolysis or ADP release, respectively, would presumably be required to achieve the ideal kinetic balance (*55*).

Physical Basis for Stimulation of ATP Hydrolysis. Two nonmutually exclusive models explain the stimulation of DnaK's ATP hydrolysis rate by DnaJ. In model 1, DnaJ accelerates ATP hydrolysis by participating directly in the chemical transformation. Presumably, this would involve one or more amino acids of DnaJ contacting ATP bound at the active site of DnaK and stabilizing developing negative charge in the transition state. Indeed, this type of mechanism has been demonstrated for an unrelated multiprotein system that has several functional similarities to the Hsp70 system. The GTP hydrolysis rate of signaling proteins in the Ras superfamily is stimulated by activating proteins (GAPs) that insert arginine residues into the GTPase active site (*56*, *57*). It is notable, however, that these GAPs stimulate GTP hydrolysis by a second means as well. Besides participating in the chemical step directly, the GAPs also affect the conformation of Ras, stabilizing portions of the Ras structure that are thought to be critically involved in the conformational changes associated with GTP hydrolysis (*56*, *57*) [see Sprang (*58*) for a recent review]. Likewise, stabilization of a specific DnaK conformation required for ATP hydrolysis would provide an alternative mechanism (model 2) to explain DnaJ's stimulatory effects.

For several reasons, direct participation of DnaJ-like proteins in ATP hydrolysis seems unlikely. Unlike GTP bound to Ras, ATP bound to Hsp70 is buried within a deep cleft with little accessibility to solvent (*15*). Without major structural rearrangements, it is difficult to imagine direct contacts between ATP and the J-domain, the region of DnaJ absolutely needed for stimulation of ATP hydrolysis. Furthermore, the solution structure of the J-domain has shown it to be compact and lacking obvious candidates for a protruding finger (*59*). Finally, peptides stimulate ATP hydrolysis by Hsp70 proteins, despite binding to a structural domain distinct from the ATP binding domain. Thus, there is little doubt that at least some stabilization of the transition state can be accomplished without direct participation in the hydrolysis reaction.

A Kinetic Model for DnaJ-Mediated Specificity. In several well-characterized examples, DnaJ is capable of binding with high affinity to a polypeptide or polypeptide complex upon which DnaK subsequently acts (*11*, *29*−*31*). For example, during the initiation of phage λ DNA replication, DnaJ binds to a nucleoprotein complex consisting of λ O and P replication proteins, *E. coli* DnaB helicase, and *ori*λ DNA (*11*, *29*). This DnaJ-containing preinitiation complex can be isolated by size-exclusion chromatography. The subsequent addition of DnaK·ATP (along with other proteins required for priming and DNA chain elongation) allows DNA replication to proceed. These and other results have led to a model in which DnaJ serves as a specificity factor for DnaK by binding specific substrates and targeting DnaK to these substrates. Such a mechanism is likely to serve as a general paradigm for Hsp70 action. For example, various eukaryotic DnaJ homologues have been shown to interact with Hsp70 proteins and either demonstrated to bind specific substrates (*43*) or found to be localized at intracellular membranes as part of a protein complex involved in polypeptide translocation (*60*, *61*). In either case, the DnaJ-like protein is present in high local concentration at the site of targeted action and is, most likely, serving as a specificity factor for Hsp70.

But how might DnaJ target polypeptides to which it is bound for action by DnaK? Productive binding of DnaK to a polypeptide substrate is likely to occur when DnaK hydrolyzes ATP while bound weakly to the polypeptide, resulting in the formation of a tight DnaK·ADP·P_i· polypeptide complex. To generate specificity, DnaJ must facilitate binding of DnaK·ATP to a DnaJ·polypeptide complex and stimulate subsequent ATP hydrolysis, relative to the equivalent reaction of DnaK·ATP alone with a similar but nontargeted polypeptide. DnaJ could generate specificity by affecting either or both of two steps: it could increase the affinity of DnaK·ATP for a polypeptide to which DnaJ is bound, or it could increase the ATP hydrolysis rate specifically in response to the targeted polypeptide. We

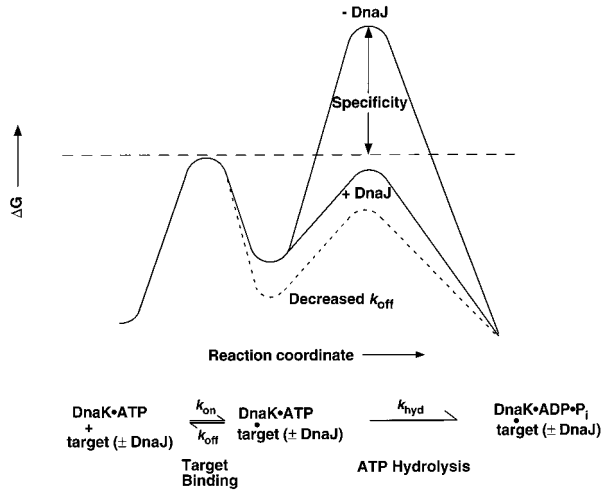

FIGURE 6: A model for generation of specificity of Hsp70 (DnaK) action by DnaJ. When DnaJ is bound to a target protein, the rate of ATP hydrolysis by DnaK is greatly accelerated when DnaK interacts with DnaJ while bound to the same target polypeptide (curve labeled "+DnaJ"). The difference in free energy barrier height in the presence and absence of DnaJ is representative of the specificity imparted. The magnitude of the rate acceleration may be sufficient to lower the free energy barrier for ATP hydrolysis to roughly the same level as that for release of DnaK·ATP from the target polypeptide. The specificity then reaches a maximum as the rate-limiting step changes from ATP hydrolysis to the binding of DnaK to the target polypeptide (horizontal dashed line). Further increases in the ATP hydrolysis rate, or in the affinity of DnaK for target polypeptides through reductions in the dissociation rate (dashed curve), would yield no further improvement of specificity, because the rate-limiting polypeptide binding step precedes these other steps.

suggest that much of the specificity imparted by DnaJ arises directly from the enormous increase in the ATP hydrolysis rate of DnaK, rather than by an increase in the affinity of DnaK for targeted polypeptides, as explained below.

The free energy barrier for formation of a productive (i.e., tight) complex between DnaK·ATP and a polypeptide involves two steps: binding of DnaK·ATP to the polypeptide and ATP hydrolysis (Figure 6). In the absence of DnaJ, DnaK·ATP dissociates from polypeptides much faster than ATP is hydrolyzed (*18*, *20*, *27*), a situation that we depict with a higher free energy barrier for ATP hydrolysis than for polypeptide binding (−DnaJ profile in Figure 6). DnaJ could generate specificity by increasing the hydrolysis rate (k_{hyd}) to lower the highest free energy barrier (+DnaJ profile in Figure 6). The large acceleration of ATP hydrolysis reported here strongly suggests that this indeed is one mechanism by which specificity is obtained. Additionally, DnaJ could generate specificity by decreasing the dissociation rate of DnaK·ATP from a targeted polypeptide (k_{off}) to stabilize both the complex and the subsequent transition state for ATP hydrolysis (dashed curve, Figure 6). A reasonable way for DnaJ to decrease k_{off} would be to supply additional binding interactions in a ternary complex with a targeted polypeptide and DnaK·ATP.

However, there is a theoretical limit to the amount of specificity that can be generated by increases in k_{hyd} or decreases in k_{off}. For example, once k_{hyd} becomes larger than k_{off}, ATP is hydrolyzed essentially every time DnaK·ATP binds the targeted polypeptide. Under these conditions, the highest free energy barrier is for binding the target polypeptide (horizontal dashed line in Figure 6), so no further increases in specificity can be generated by effects on k_{hyd} or k_{off}. Strikingly, this theoretical limit appears to be reached solely as a consequence of the DnaJ-mediated increase in ATP hydrolysis rate (+DnaJ profile in Figure 6), since the maximum value of the k_{hyd} rate constant observed here is similar to, or even larger than, previously reported values for dissociation of DnaK·ATP from various polypeptides (*18*, *20*, *62*). A decrease in k_{off}, when accompanied by an increased k_{hyd} (dashed curve in Figure 6), would not result in enhanced specificity because target binding is already rate-limiting under these conditions. Nevertheless, it is likely that the presence of DnaJ in a ternary complex of DnaK·ATP and a target *does* lead to a decreased k_{off}, since DnaJ, by definition in this model, interacts with both DnaK and polypeptide.

Although decreases in k_{off} would not be expected to enhance specificity, it is possible that DnaJ additionally enhances specificity by increasing k_{on}, the rate constant for target binding by DnaK·ATP. One possibility is that DnaJ binding may induce conformational changes in the target that expose a previously hidden DnaK binding site. The available kinetic evidence indicates that peptide binding to DnaK·ATP is relatively slow (*18*, *62*), 3−4 orders of magnitude below the expected encounter frequency (*51*), so there clearly is opportunity for DnaJ to facilitate this step. Nevertheless, the large size of the increase in ATP hydrolysis rate suggests that DnaJ achieves much of its specificity directly from this increase, by binding to target sites and transiently interacting with a DnaK·ATP·polypeptide complex to elicit ATP hydrolysis from DnaK. In the absence of DnaJ, DnaK·ATP binds and releases a polypeptide many times before ATP is hydrolyzed to yield a productive complex. In contrast, the binding interaction of DnaJ with the target serves to effectively localize the J-domain to a position where it can trigger ATP hydrolysis essentially every time DnaK interacts with the target polypeptide. This model has received support in a recent study (*63*), published after submission of this article. Misselwitz et al. have demonstrated that the yeast Sec63p J-domain catalytically activates yeast Kar2p (BiP), an ER-resident Hsp70 family member, to bind to peptides or proteins that Kar2p does not bind stably on its own. Because the J-domain apparently does not itself interact with targeted polypeptides, this result suggests further that DnaJ proteins also can provide substrate specificity without binding directly to the target polypeptide, presumably acting through the kinetic mechanism proposed above. In a similar fashion, isolated J-domain has been previously shown to activate binding of DnaK to the σ^{32} heat shock transcriptional regulator (*64*).

Other observations support this kinetic model for substrate specificity, which has some similarities to a model recently reported by Pierpaoli et al. (*55*), and suggest that the model may be broadly applicable to Hsp70 action. First, the K_D for the association of DnaJ and DnaK·ATP is $>20\ \mu$M. This, along with other evidence, indicates that this binding interaction is in rapid equilibrium, consistent with the idea that DnaJ does not recruit DnaK by virtue of a high-affinity interaction. It may, in fact, be advantageous for DnaJ to have a relatively low affinity for DnaK·ATP. Stable association of the two in solution would lead to ATP hydrolysis by DnaK, presumably a futile reaction in the absence of a

polypeptide substrate. In several cases, it has been shown that ATP is required for the detection of a complex between Hsp70s and DnaJ-like proteins (*45*, *53*, *65*); however, further analysis has shown that the nucleotide is primarily ADP in such a complex (*45*). This is consistent with a low affinity of Hsp70·ATP for DnaJ-like proteins and with tighter binding following rapid ATP hydrolysis.

The magnitude of the DnaJ-mediated stimulatory effect on ATP hydrolysis may also be general. Though there are no other published reports estimating the total rate enhancement by any DnaJ homologue, the steady-state ATPase activity of some eukaryotic Hsp70s has been shown to become limited by ADP release in the presence of DnaJ homologues [e.g., (*66*)]. This similarity to the situation for DnaK and DnaJ, demonstrated in this report, leaves open the possibility that the ATP hydrolysis rate-enhancement by eukaryotic DnaJ homologues could be comparable to the 15 000-fold stimulation reported here for DnaJ.

ACKNOWLEDGMENT

We thank Dr. Cecile Pickart for a critical review of the manuscript and for helpful discussions.

REFERENCES

1. Deshaies, R. J., Koch, B. D., Werner-Washburne, M., Craig, E. A., and Schekman, R. (1988) *Nature 332*, 800−805.
2. Chirico, W. J., Waters, M. G., and Blobel, G. (1988) *Nature 332*, 805−810.
3. Straus, D. B., Walter, W. A., and Gross, C. A. (1988) *Genes Dev. 2*, 1851−1858.
4. Straus, D., Walter, W., and Gross, C. A. (1990) *Genes Dev. 4*, 2202−2209.
5. Nelson, R. J., Ziegelhoffer, T., Nicolet, C., Werner-Washburne, M., and Craig, E. A. (1992) *Cell 71*, 97−105.
6. Hartl, F. U. (1996) *Nature 381*, 571−579.
7. Bukau, B., and Horwich, A. L. (1998) *Cell 92*, 351−366.
8. Ungewickell, E. (1985) *EMBO J. 4*, 3385−3391.
9. Chappell, T. G., Welch, W. J., Schlossman, D. M., Palter, K. B., Schlesinger, M. J., and Rothman, J. E. (1986) *Cell 45*, 3−13.
10. Alfano, C., and McMacken, R. (1989) *J. Biol. Chem. 264*, 10709−10718.
11. Zylicz, M., Ang, D., Liberek, K., and Georgopoulos, C. (1989) *EMBO J. 8*, 1601−1608.
12. Wickner, S., Hoskins, J., and McKenney, K. (1991) *Proc. Natl. Acad. Sci. U.S.A. 88*, 7903−7907.
13. Landry, S. J., Jordan, R., McMacken, R., and Gierasch, L. M. (1992) *Nature 355*, 455−457.
14. Zhu, X., Zhao, X., Burkholder, W. F., Gragerov, A., Ogata, C. M., Gottesman, M. E., and Hendrickson, W. A. (1996) *Science 272*, 1606−1614.
15. Flaherty, K. M., DeLuca-Flaherty, C., and McKay, D. B. (1990) *Nature 346*, 623−628.
16. Montgomery, D., Jordan, R., McMacken, R., and Freire, E. (1993) *J. Mol. Biol. 232*, 680−692.
17. Ha, J. H., and McKay, D. B. (1994) *Biochemistry 33*, 14625−14635.
18. Schmid, D., Baici, A., Gehring, H., and Christen, P. (1994) *Science 263*, 971−973.
19. Takeda, S., and McKay, D. B. (1996) *Biochemistry 35*, 4636−4644.
20. Theyssen, H., Schuster, H. P., Packschies, L., Bukau, B., and Reinstein, J. (1996) *J. Mol. Biol. 263*, 657−670.
21. McCarty, J. S., Buchberger, A., Reinstein, J., and Bukau, B. (1995) *J. Mol. Biol. 249*, 126−137.
22. Russell, R., Jordan, R., and McMacken, R. (1998) *Biochemistry 37*, 596−607.
23. Jordan, R., and McMacken, R. (1995) *J. Biol. Chem. 270*, 4563−4569.
24. Greene, L. E., Zinner, R., Naficy, S., and Eisenberg, E. (1995) *J. Biol. Chem. 270*, 2967−2973.
25. Palleros, D. R., Reid, K. L., Shi, L., Welch, W. J., and Fink, A. L. (1993) *Nature 365*, 664−666.
26. Liberek, K., Marszalek, J., Ang, D., Georgopoulos, C., and Zylicz, M. (1991) *Proc. Natl. Acad. Sci. U.S.A. 88*, 2874−2878.
27. Karzai, A. W., and McMacken, R. (1996) *J. Biol. Chem. 271*, 11236−11246.
28. Packschies, L., Theyssen, H., Buchberger, A., Bukau, B., Goody, R. S., and Reinstein, J. (1997) *Biochemistry 36*, 3417−3422.
29. Alfano, C., and McMacken, R. (1989) *J. Biol. Chem. 264*, 10699−10708.
30. Wickner, S. H. (1990) *Proc. Natl. Acad. Sci. U.S.A. 87*, 2690−2694.
31. Gamer, J., Bujard, H., and Bukau, B. (1992) *Cell 69*, 833−842.
32. Kudlicki, W., Odom, O. W., Kramer, G., and Hardesty, B. (1996) *J. Biol. Chem. 271*, 31160−31165.
33. Cyr, D. M., Lu, X., and Douglas, M. G. (1992) *J. Biol. Chem. 267*, 20927−20931.
34. Brodsky, J. L., and Schekman, R. (1993) *J. Cell Biol. 123*, 1355−1363.
35. Scidmore, M. A., Okamura, H. H., and Rose, M. D. (1993) *Mol. Biol. Cell 4*, 1145−1159.
36. Becker, J., Walter, W., Yan, W., and Craig, E. A. (1996) *Mol. Cell. Biol. 16*, 4378−4386.
37. Wall, D., Zylicz, M., and Georgopoulos, C. (1994) *J. Biol. Chem. 269*, 5446−5451.
38. Sadler, I., Chiang, A., Kurihara, T., Rothblatt, J., Way, J., and Silver, P. (1989) *J. Cell Biol. 109*, 2665−2675.
39. Brodsky, J. L., Goeckeler, J., and Schekman, R. (1995) *Proc. Natl. Acad. Sci. U.S.A. 92*, 9643−9646.
40. Lyman, S. K., and Schekman, R. (1995) *J. Cell Biol. 131*, 1163−1171.
41. Banecki, B., Liberek, K., Wall, D., Georgopoulos, C., Bertoli, E., Tanfani, F., and Zylicz, M. (1996) *J. Biol. Chem. 271*, 14840−14848.
42. Szabo, A., Korszun, R., Hartl, F. U., and Flanagan, J. (1996) *EMBO J. 15*, 408−417.
43. Ungewickell, E., Ungewickell, H., Holstein, S. E., Lindner, R., Prasad, K., Barouch, W., Martin, B., Greene, L. E., and Eisenberg, E. (1995) *Nature 378*, 632−635.
44. Silver, P. A., and Way, J. C. (1993) *Cell 74*, 5−6.
45. Holstein, S. E., Ungewickell, H., and Ungewickell, E. (1996) *J. Cell Biol. 135*, 925−937.
46. Gill, S. C., and von Hippel, P. H. (1989) *Anal. Biochem. 182*, 319−326.
47. Johnson, K. A. (1995) *Methods Enzymol. 249*, 38−61.
48. Johnson, K. A. (1986) *Methods Enzymol. 134*, 677−705.
49. Fersht, A. (1985) in *Enzyme structure and mechanism*, W. H. Freeman and Co., New York.
50. Ha, J. H., and McKay, D. B. (1995) *Biochemistry 34*, 11635−11644.
51. Eigen, M., and Hammes, G. G. (1963) *Adv. Enzymol. Relat. Areas Mol. Biol. 25*, 1−38.
52. Slepenkov, S. V., and Witt, S. N. (1998) *Biochemistry 37*, 1015−1024.
53. Jiang, R. F., Greener, T., Barouch, W., Greene, L., and Eisenberg, E. (1997) *J. Biol. Chem. 272*, 6141−6145.
54. Pierpaoli, E. V., Sandmeier, E., Baici, A., Schonfeld, H. J., Gisler, S., and Christen, P. (1997) *J. Mol. Biol. 269*, 757−768.
55. Pierpaoli, E. V., Sandmeier, E., Schonfeld, H. J., and Christen, P. (1998) *J. Biol. Chem. 273*, 6643−6649.
56. Scheffzek, K., Ahmadian, M. R., Kabsch, W., Wiesmnller, L., Lautwein, A., Schmitz, F., and Wittinghofer, A. (1997) *Science 277*, 333−338.
57. Rittinger, K., Walker, P. A., Eccleston, J. F., Smerdon, S. J., and Gamblin, S. J. (1997) *Nature 389*, 758−762.
58. Sprang, S. R. (1997) *Curr. Opin. Struct. Biol. 7*, 849−856.

59. Szyperski, T., Pellecchia, M., Wall, D., Georgopoulos, C., and Wuthrich, K. (1994) *Proc. Natl. Acad. Sci. U.S.A. 91*, 11343−11347.
60. Feldheim, D., Rothblatt, J., and Schekman, R. (1992) *Mol. Cell. Biol. 12*, 3288−3296.
61. Rowley, N., Prip-Buus, C., Westermann, B., Brown, C., Schwarz, E., Barrell, B., and Neupert, W. (1994) *Cell 77*, 249−259.
62. Gisler, S. M., Pierpaoli, E. V., and Christen, P. (1998) *J. Mol. Biol. 279*, 833−840.
63. Misselwitz, B., Staeck, O., and Rapoport, T. A. (1998) *Mol. Cell 2*, 593−603.
64. Liberek, K., Wall, D., and Georgopoulos, C. (1995) *Proc. Natl. Acad. Sci. U.S.A. 92*, 6224−6228.
65. Wawrzynow, A., and Zylicz, M. (1995) *J. Biol. Chem. 270*, 19300−19306.
66. Cheetham, M. E., Jackson, A. P., and Anderton, B. H. (1994) *Eur. J. Biochem. 226*, 99−107.

BI9824036